



Received 21 May 2020 Accepted 20 July 2020

Edited by M. Zeller, Purdue University, USA

Keywords: lanthanide; rare earth; diphenylamide; oxide; crystal structure.

CCDC references: 2017774; 2017773; 2017772; 2017771; 2017770

Supporting information: this article has supporting information at journals.iucr.org/e

Synthesis and crystallographic characterization of diphenylamide rare-earth metal complexes *n* NPh₂)₃ THF)₂ and [Ph₂N)₂ *n* μ -NPh₂)]₂

Chad T. Palumbo, Christopher M. Kotyk, Joseph W. Ziller and William J. Evans*

Department of Chemistry, University of California, Irvine, CA 92697-2025, USA. *Correspondence e-mail: wevans@uci.edu

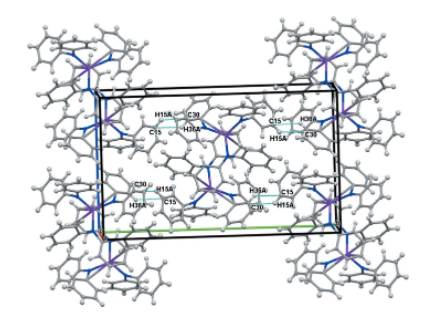
Studies of the coordination chemistry between the diphenylamide ligand, NPh₂, and the smaller rare-earth Ln^{III} ions, Ln = Y, Dy, and Er, led to the structural characterization by single-crystal X-ray diffraction crystallography of both solvated and unsolvated complexes, namely, tris(diphenylamido- κN)bis(tetrahydrofuran- κO)yttrium(III), $Y(NPh_2)_3(THF)_2$ or $[Y(C_{12}H_{10}N)_3(C_4H_8O)_2]$, **1-Y**, and the erbium(III) (Er), **1-Er**, analogue, and bis μ -1 κN :2(η^6)-diphenylamido]bis[bis(diphenylamido- κN)yttrium(III)], $[(Ph_2N)_2Y(\mu-NPh_2)]_2$ $[Y_2(C_{12}H_{10}N)_6]$, **2-Y**, and the dysprosium(III) (Dy), **2-Dy**, analogue. The THF ligands of 1-Er are modeled with disorder across two positions with occupancies of 0.627 (12):0.323 (12) and 0.633 (7):0.367 (7). Also structurally characterized was the tetrametallic Er^{III} bridging oxide hydrolysis product, bis(μ -diphenylamido- $\kappa^2 N:N$)bis[μ -1 $\kappa N:2(\eta^6)$ -diphenylamido]tetrakis(diphenylamido- κN)di- μ_3 -oxido-tetraerbium(III) benzene disolvate, {[(Ph₂N)Er(μ -NPh₂)]₄(μ - O_{2} ($C_{6}H_{6}$)₂ or $[Er_{4}(C_{12}H_{10}N)_{8}O_{2}]$ 2 $C_{6}H_{6}$, 3-Er. The 3-Er structure was refined as a three-component twin with occupancies 0.7375:0.2010:0.0615.

1. Chemical context

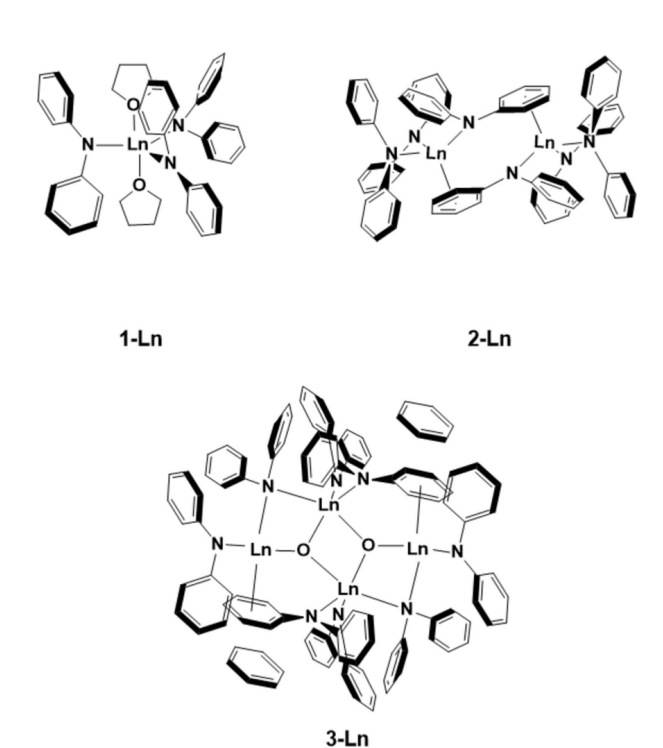
Although the amide ligand, NR_2 , is widely used in rare-earth metal chemistry, most studies involve the bis(trimethylsil-yl)amide ligand originally introduced by Bradley, $N(SiMe_3)_2$ (Alyea *et al.*, 1972; Bradley *et al.*, 1972, 1973), and the dimethylsilyl analog, $N(SiHMe_2)_2$ (Anwander *et al.*, 1998; Bienfait *et al.*, 2014; Meermann *et al.*, 2008), developed by Anwander. The neutral homoleptic complexes, $Ln[N(SiMe_3)_2]_3$ and $Ln[N(SiHMe_2)_2]_3(THF)_2$, are heavily used in the rare-earth field.

In comparison, the NPh₂ ligand has not been as extensively explored. The only neutral crystallographically characterized NPh₂ rare-earth metal complexes in the literature are Yb(NPh₂)₃(THF)₂ (**1-Yb**) (Yao *et al.*, 2001), Yb(NPh₂)₃-[OP(NMe₂)₃]₂ (Xu *et al.*, 2007), and $[(Ph_2N)_2Ce(\mu-NPh_2)]_2$ (**2-Ce**) (Coles *et al.*, 2010). Many of the rare-earth NPh₂ species are complex anions such as $[Ln(NPh_2)_4]^{1-}$ (Yao *et al.*, 2004; Wong *et al.*, 1997*a,b*; Yu *et al.*, 2016), $[Ln(NPh_2)_4]^{2-}$ (Minhas *et al.*, 1996), and $[(C_5H_4R)Ln(NPh_2)_3]^{1-}$ (R = Me, ^tBu) (Mao *et al.*, 1994).

To remedy the dearth of structural information on this class, we report the structures shown in the Scheme of the THF-solvated monometallic complexes $Ln(\mathrm{NPh_2})_3(\mathrm{THF})_2$, **1-Ln** $(Ln=Y,\mathrm{Er})$, the unsolvated bimetallic complexes $[(\mathrm{Ph_2N})_2Ln(\mu\text{-NPh_2})]_2$, **2-Ln** $(Ln=Y,\mathrm{Dy})$, and the tetrametallic hydrolysis product $\{[(\mathrm{Ph_2N})\mathrm{Er}(\mu\text{-NPh_2})]_4(\mu\text{-O})_2\}$ - $(C_6H_6)_2$, **3-Er**.

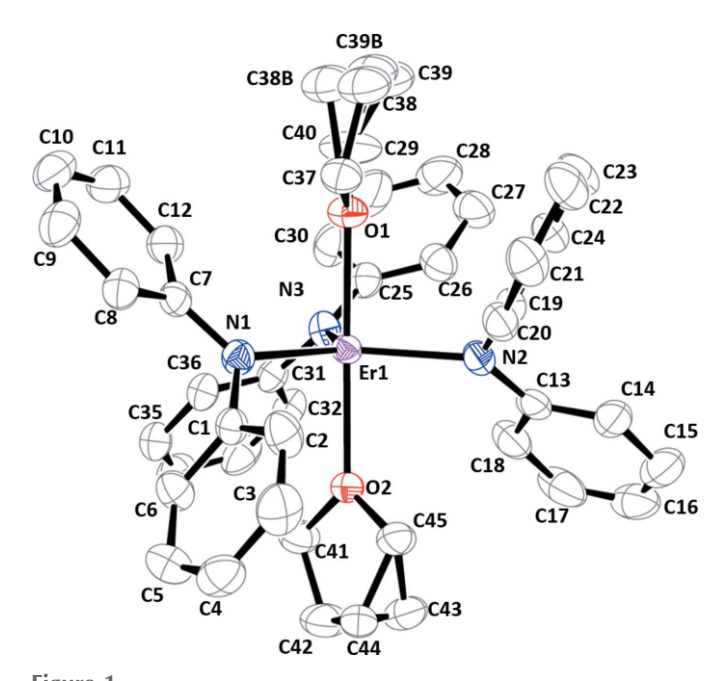






2. Structural commentary

Monometallic Complexes. The metrical parameters of the $Ln(NPh_2)_3(THF)_2$ complexes, **1-Ln** (Ln = Y, Er), are shown in Table 1 and the displacement ellipsoid plot of **1-Er** is shown in Fig. 1. The **1-Ln** complexes are not isomorphous; complex **1-Y** crystallizes in the $P2_1/c$ space group and **1-Er** in $P2_1/n$. They



Displacement ellipsoid plot of Er(NPh₂)₃(THF)₂, **1-Er**, drawn at the 50% probability level. Hydrogen atoms and co-crystallized solvent molecules are omitted for clarity.

Table 1 Selected bond distances (Å) and angles ($^{\circ}$) of $Ln(NPh_2)_3(THF)_2$, **1-Ln**.

Parameter	1-Y	1-Er	
Ln1-N1	2.2612 (14)	2.2733 (15)	
Ln1-N2	2.2399 (14)	2.2524 (15)	
Ln1-N3	2.2870 (14)	2.2344 (15)	
Ln1-N(amide)avg	2.26 (2)	2.25 (2)	
Ln1-O1	2.3526 (11)	2.3475 (12)	
Ln1-O2	2.3838 (12)	2.3353 (11)	
Ln1-O(THF)avg	2.37 (2)	2.342 (6)	
N1-Ln1-N2	106.77 (5)	130.04 (6)	
N1-Ln1-N3	130.61 (5)	119.13 (5)	
N2-Ln1-N3	122.03 (5)	110.83 (6)	
O1-Ln1-O2	160.31 (4)	167.72 (4)	

contain five-coordinate Ln^{III} ions with three amide and two neutral THF ligands arranged in a distorted trigonal-bipyramidal geometry. The divergence from perfect trigonal bipyramidal is evident by the three N(amide)-Ln1-N(amide) bond angles [1-Y: 130.61 (5), 122.03 (5), and 106.77 (5)°; **1-Er**: 130.04 (6), 119.13 (5), and 110.83 (6)°] that deviate from 120° and the O1-Ln1-O2 bond angles [1-Y: $160.31 (4)^{\circ}$; **1-Er**: $167.72 (4)^{\circ}$] that deviate from linearity. Complex **1-Y** has a τ_5 parameter (Addison *et al.*, 1984) of 0.50 indicating a geometry halfway between ideal square-pyramidal ($\tau_5 = 0$) and trigonal–bipyramidal ($\tau_5 = 1$). The τ_5 value of 1-Er is 0.63 suggesting a geometry closer to trigonalbipyramidal. The $Ln-N(amide)_{avg}$ bond distances are 2.26(2) Å for 1-Y [Y1-N1 = 2.2612(14), Y1-N2 =2.2399 (14), Y1-N3 = 2.2870 (14) Å and 2.25 (2) Å for**1-Er** [Er1-N1 = 2.2733 (15), Er1-N2 = 2.2524 (15), Er1-N3 =2.2344 (15) Å], which reflects the similar size of these two ions [six-coordinate ionic radii: Y(III), 0.9 Å; Er(III), 0.89 Å] (Shannon, 1976). The $Ln-O(THF)_{avg}$ bond lengths are 2.37 (2) Å for 1-Y [Y1-O1 = 2.3526 (11), Y1-O2 =2.3838 (12) Å and 2.342 (6) Å for **1-Er** [Er1-O1 = 2.3475 (12), Er2-O2 = 2.3353 (11) Å].

Bimetallic Complexes. The metrical parameters of $[(Ph_2N)_2Ln(\mu-NPh_2)]_2$, **2-Ln** (Ln = Y, Dy), are presented in Table 2 and the displacement ellipsoid plot of **2-Dy** is in Fig. 2.

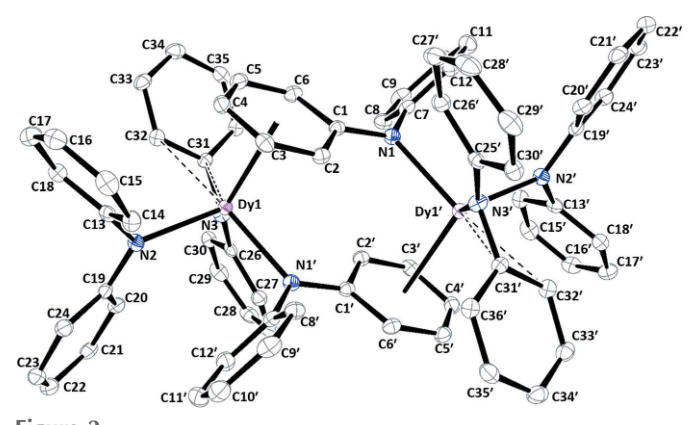


Figure 2 Displacement ellipsoid plot of $[(Ph_2N)_2Dy(\mu-NPh_2)]_2$, **2-Dy**, drawn at the 50% probability level. Hydrogen atoms are omitted for clarity. The dashed lines represent the Ln-C(ortho) and Ln-C(ipso) distances discussed in the text. Symmetry code: (')-x+1,-y+1,-z+1.

Table 2 Selected bond distances (Å) and angles (°) of $[(Ph_2N)_2Ln(\mu-NPh_2)]_2$, 2-Ln

Parameter	2-Y	2-Dy	
Ln1-N1'	2.3039 (15)	2.309 (2)	
Ln1-N2	2.2294 (15)	2.228 (2)	
Ln1-N3	2.2340 (15)	2.240(2)	
Ln1-N(amide)avg	2.25 (3)	2.26 (4)	
Ln1-C1	3.1300 (18)	3.151 (2)	
Ln1-C2	2.9498 (18)	2.967 (2)	
Ln1-C3	2.8400 (18)	2.858 (2)	
Ln1-C4	2.8129 (19)	2.833 (2)	
Ln1-C5	2.8898 (18)	2.904 (3)	
Ln1-C6	3.0125 (19)	3.032 (3)	
<i>Ln</i> 1—Centroid(phenyl)	2.584	2.605	
Ln1-C31	2.8235 (17)	2.836 (2)	
Ln1-C32	3.0169 (18)	3.033	

Symmetry code: (') -x + 1, -y + 1, -z + 1.

The two **2-Ln** complexes (Ln = Y and Dy) are isomorphous and crystallize in the monoclinic $P2_1/c$ space group. Each molecule of **2-Ln** is a dimer comprised of two $(Ph_2N)_2Ln(\mu$ -NPh₂) units that are related by an inversion center. The $(\mu\text{-NPh}_2)$ ligand involving atom N1 binds to one lanthanide center through the nitrogen atom and links to the other lanthanide center via η^6 coordination of one of the phenyl rings. The terminal NPh₂ ligand involving N2 binds just through the nitrogen donor atom. The other terminal NPh₂ ligand containing N3 attaches to the Ln atom through the nitrogen, but it also has a phenyl ring oriented toward the metal with Ln-C(ipso) and Ln-C(ortho) distances of 2.8235 (17) and 3.0169 (18) Å for Y and 2.836 (2) and 3.033 Å for Dy. These distances can be compared with the Ln1-N3 distances in these complexes: 2.2340 (15) Å for Y and 2.240 (2) Å for Dy. The bond distances of 2-Y and 2-Dy are close, which is consistent with their similar Shannon (1976) ionic radii [six-coordinate ionic radii: Y(III), 0.9 Å; Dv(III), 0.912 Å].

The 2.228 (2)–2.240 (2) Å range of terminal Ln–N(amide) bond distances in **2-Ln** is at the lower end of the 2.2343 (15)–2.2870 (14) Å range of distances in **1-Ln** and slightly shorter than the Ln–N1 distances of the bridging NPh₂ [Y1–N1' = 2.3039 (15) and Dy1–N1' = 2.309 (2) Å], as is typical for

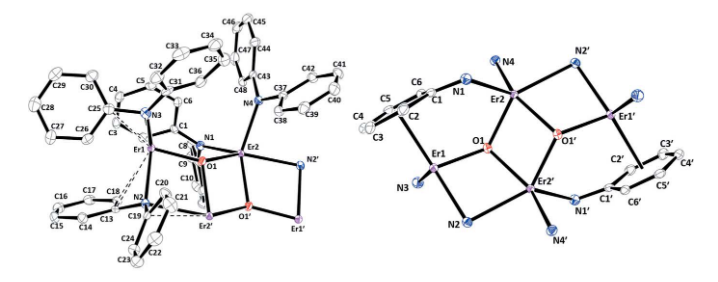


Figure 3 Displacement ellipsoid plots drawn at the 50% probability level of the asymmetric unit of $\{[(Ph_2N)Er(\mu-NPh_2)]_4(\mu-O)_2\}$ (C_6H_6)₂, **3-Er**, with atoms Er1′, Er2′, O1′, N2′ added for clarity (left) and the Er₄O₂ core of **3-Er** (right). Hydrogen atoms and a molecule of benzene in the asymmetric unit are omitted for clarity. Symmetry code: (′) -x + 1, -y + 1, -z + 1.

Table 3 Selected bond distances (Å) and angles (°) of $\{[(Ph_2N)Er(\mu-NPh_2)]_4(\mu-O)_2\}$ (C_6H_6)₂, 3-Er.

Parameter	3-Er
Er1-O1	2.095 (3)
Er2-O1	2.190 (3)
Er2-O1'	2.245 (3)
Er1-N2	2.367 (4)
Er1-N3	2.222 (3)
Er2-N1	2.303 (3)
Er2-N4	2.313 (4)
Er1-C1	2.871 (4)
Er1-C2	2.988 (4)
Er1-C3	2.989 (4)
Er1-C4	2.884 (4)
Er1-C5	2.784 (4)
Er1-C6	2.761 (4)
Er1—Centroid(phenyl)	2.516
Er1-C13	2.812 (4)
Er1-C18	2.805 (4)
Er1-C25	2.904 (4)
Er2-C19'	2.903 (4)
Er1-O1-Er2	133.25 (14)
Er1-O1-Er2'	110.82 (12)
Er2-O1-Er2'	103.54 (11)
Er1 Er2'	3.5734 (3)
Er2 Er2'	3.4836 (4)

Symmetry code: (') -x + 1, -y + 1, -z + 1.

terminal vs bridging ligands. The Ln-N2 distances [Y, 2.2294 (15) Å; Dy 2.228 (2) Å] are similar and comparable to the Ln-N1 bond lengths. The Ln-(phenyl ring centroid distances are also similar [Y, 2.584 Å; Dy, 2.605 Å] with similar Ln-C(phenyl) bond distance ranges [Y, 2.8129 (19)–3.1300 (18) Å; Dy, 2.833 (2)–3.151 (3) Å].

A Tetrametallic Complex. The displacement ellipsoid plot and metrical parameters of $\{[(Ph_2N)Er(\mu-NPh_2)]_4(\mu-O)_2\}$ - $(C_6H_6)_2$, **3-Er**, are shown below in Figs. 3 and 4 and Table 3.

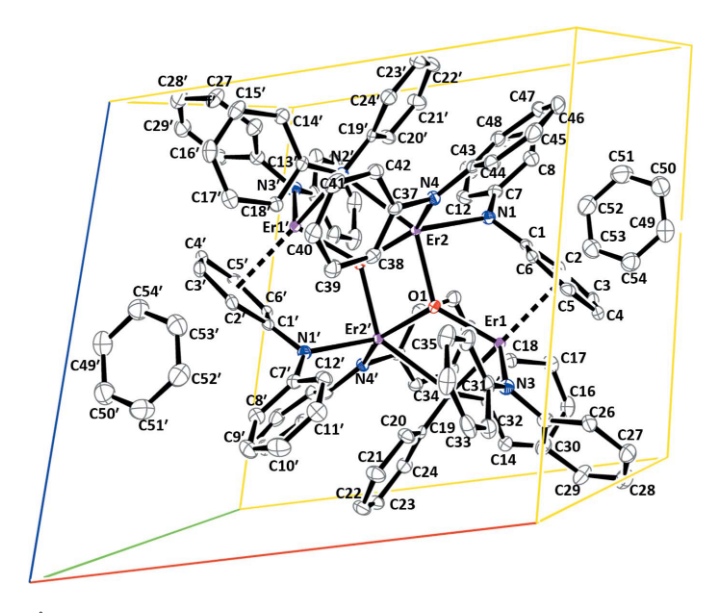


Figure 4 Unit-cell contents of {[(Ph₂N)Er(μ -NPh₂)]₄(μ -O)₂} (C₆H₆)₂, **3-Er**, with displacement ellipsoids drawn at the 50% probability level. Hydrogen atoms are omitted for clarity. Symmetry code: (') -x + 1, -y + 1, -z + 1.

research communications

Table 4
Intermolecular contact lengths (Å) in 1-Y.

vdW indicates the sum of the van der Waals radii of the two atoms.

Contact	1-Y	Length - vdW
C5 C21	3.388	-0.012
C5 H41A	2.840	-0.060
C6 H33A	2.890	-0.010
C18 H5A	2.822	-0.078
C33 H40B	2.825	-0.075
H8A H20A	2.391	-0.009
H18A H18A'	2.275	-0.125
H33A H40B	2.271	-0.129
H34A H40A	2.370	-0.030

Table 5 Intermolecular contact lengths (Å) in 1-Er.

vdW indicates the sum of the van der Waals radii of the two atoms.

Contact	1-Er	Length - vdW	
C8 H23	2.873	-0.027	
C14 H21	2.835	-0.065	
C21 H45 <i>B</i>	2.897	-0.003	

Complex **3-Er** crystallizes in the triclinic $P\overline{1}$ space group and is a tetrametallic complex of Er^{III} comprised of two symmetrical $\{[(Ph_2N)Er(\mu-NPh_2)]_2(\mu-O)\}$ (C_6H_6) units. The coordination environments of the two Er^{III} ions in this unit are different, as are all four NPh_2 ligands. Er2 is five-coordinate with two μ -O bonds and three Er-N bonds. The bonding to Er1 is more complicated. It is bound to one μ -O ligand and one terminal NPh_2 ligand through N3 with a short distance to ipso carbon C25. Er1 is also bound η^6 to a phenyl group of one μ - NPh_2 ligand and to another μ - NPh_2 ligand through the N2 atom that also bridges to Er2. In addition, C13 and C18 of this μ - NPh_2 ligand are oriented toward Er1. The differences in the coordination environments of Er1 and Er2 lead to inequivalent Er-O bond distances [Er1-O1=2.095 (3), Er2-O1=2.190 (3) Å, Er2-O1'=2.245 (3) Å]. The Er-O-Er angle is

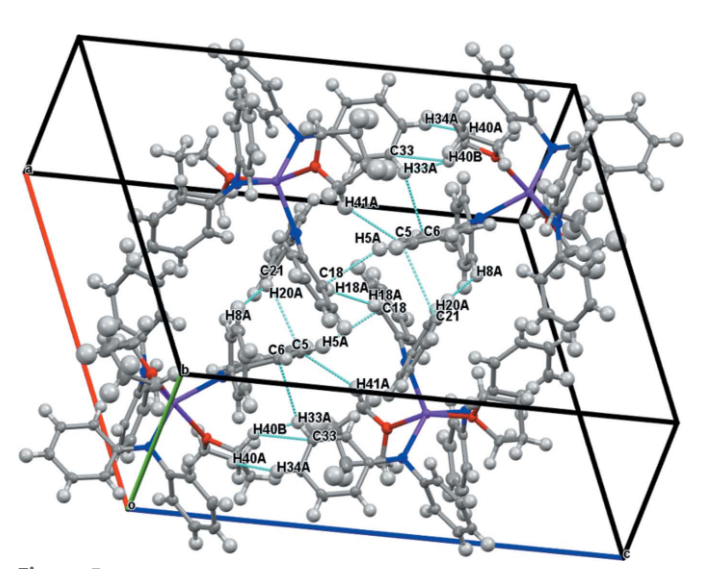


Figure 5
Packing structures and contacts for 1-Y.

Table 6
Intermolecular contact lengths (Å) in 2-Y and 2-Dy.

Contact		2-Y	Length-vdW	2-Dy	Length - vdW
C15 C30	H36 <i>A</i> H15 <i>A</i>	2.749 2.805	-0.151 -0.095	2.737 2.800	-0.163 -0.100

Table 7
Intermolecular contact lengths (Å) in 3-Er.

vdW indicates the sum of the van der Waals radii of the two atoms.

Contact		3-Er	Length - vdW	
H17A	H54A	2.370	-0.030	

bent $[Er1-O1-Er2 = 133.25 (14)^{\circ}]$. The closest distances between the Er^{III} ions are Er1 = Er2' = 3.5734 (3) Å and Er2 = Er2' = 3.4836 (4) Å.

3. Supramolecular features

An examination of the packing diagrams for **1-Ln** (Ln = Y, Er), **2-Ln** (Ln = Y and Dy), and **3-Er** shows close C—H phenyl interactions throughout the structures, Tables 4–7 and Figs. 5–8. Complex **3-Er** has two molecules of benzene in the unit cell.

4. Database survey

A search of the Cambridge Structural Database shows **1-Yb** (Yao *et al.*, 2001) and **2-Ce** (Coles *et al.*, 2010) have been reported. Complex **1-Yb** is isomorphous with **1-Er**. Complex **2-Ce** is not isomorphous with **2-Y** and **2-Dy** and crystallizes in

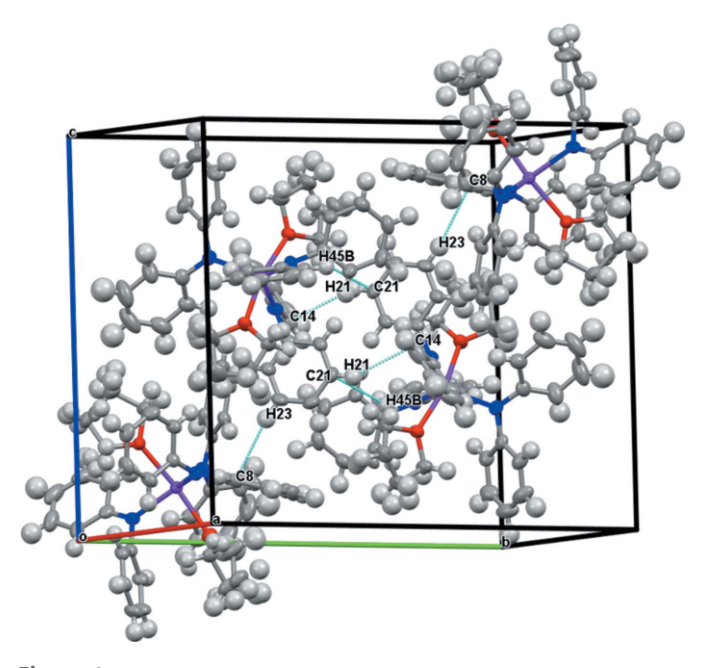


Figure 6
Packing structures and contacts for 1-Er.

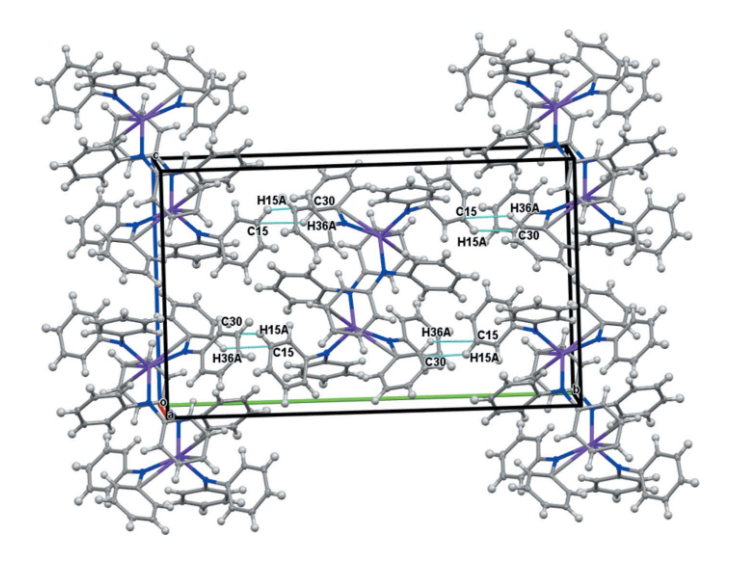


Figure 7
Packing structures and contacts for 2-Ln.

the C2/c space group. **2-Ce** is structurally different in that the μ -NPh₂ ligand bridges the two Ce atoms only through the nitrogen donor atom and not via η^6 -phenyl-coordination as observed in **2-Y** and **2-Dy**. The tris(amide) complex Yb(NPh₂)₃[OP(NMe₂)₃]₂ (Xu *et al.*, 2007) has also been reported.

5. Synthesis and crystallization

General Considerations. All manipulations and syntheses described below were conducted with rigorous exclusion of air and water using standard Schlenk line and glovebox techniques under an argon atmosphere. Solvents were sparged with UHP argon (Airgas) and dried by passage through columns containing Q-5 and molecular sieves prior to use. $LnCl_3$ was prepared from the previously reported literature

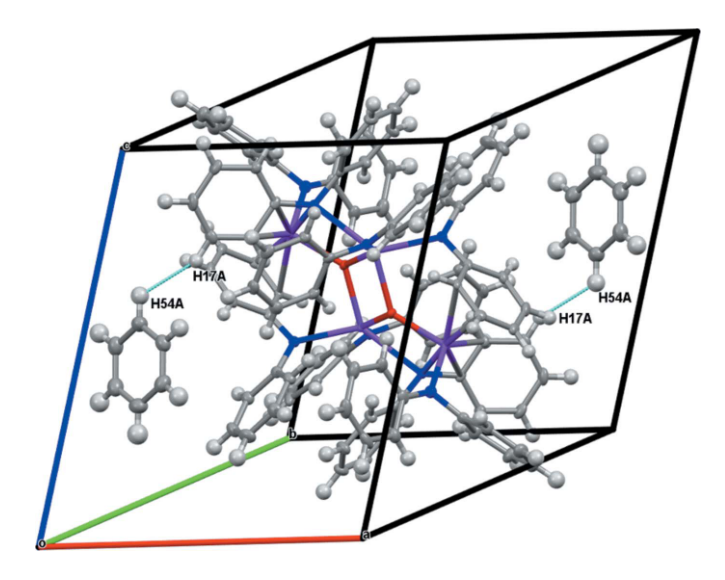


Figure 8
Packing structures and contacts for **3-Er**.

procedure (Meyer *et al.*, 1982). The compounds $Ln[N(SiMe_3)_2]_3$ were prepared from their literature procedures (Bradley *et al.*, 1972). HNPh₂ was purchased from commercial suppliers and used as received. NaNPh₂ and KNPh₂ were prepared by reaction of HNPh₂ with NaH or KH in THF.

Synthesis and Crystallization of Y(NPh₂)₃(THF)₂, 1-Y. In a glovebox, YCl₃ (0.63 g, 3.2 mmol) was stirred for two days in THF (30 mL) in a Schlenk flask to ensure complete solvation. Under positive pressure of N₂ on a Schlenk line, a solution of KNPh₂ (1.9 g, 9.1 mmol) in THF (30 mL) was added dropwise to the YCl₃ suspension in THF at 273 K over 15 min. The reaction vessel was allowed to warm to room temperature, and after 1 h, the solvent was removed under reduced pressure to yield a colorless solid. In a glovebox, the product was extracted with toluene and evaporated to dryness. The resulting solids were washed with hexane to yield 1-Y as a colorless solid (2.2 g, 90%). The colorless solid was dissolved in diethyl ether and stored at 245 K for three days to yield colorless crystals of 1-Y.

Synthesis and Crystallization of Er(NPh₂)₃(THF)₂, 1-Er. In a glovebox, ErCl₃ (243 mg, 0.887 mmol) was stirred in THF (10 mL), which gave a pink slurry. To the stirred suspension was added NaPh₂ (500 mg, 2.62 mmol) in THF (10 mL) at 238 K dropwise over 5 min, and a color change to greenyellow and then pink was observed. After the addition, the resultant pink slurry was allowed to warm to room temperature and left to stir overnight. The volatiles were then removed under reduced pressure, which gave a pink gel. The gel was triturated with hexane several times to yield pink solids that were then dissolved in Et₂O (17 mL) and stirred for several hours to ensure complete dissolution. Pink and colorless solids, presumably unreacted ErCl₃ and NaNPh₂, were centrifuged, and the volatiles of the supernatant were evaporated until supersaturation. As the concentrated pink solution warmed to room temperature, large pink hexagonshaped crystals of Er(NPh₂)₃(THF)₂, **1-Er**, suitable for X-ray diffraction grew within minutes (260 mg, 36%).

Synthesis and Crystallization of $[(NPh_2)_2Y(\mu-NPh_2)]_2$, 2-Y. In a glovebox free of coordinating solvents, $Y[N(SiMe_3)_2]_3$ (300 mg, 0.526 mmol) was dissolved in toluene (10 mL). To the stirred solution was added HNPh₂ (272 mg, 1.61 mmol) in toluene (10 mL). The resultant colorless solution was left to stir for 48 h. The color of the solution slowly changed to yellow and a yellow precipitate was observed. The volatiles were removed under vacuum, and the resultant yellow solids were washed with hexane. The solids were stirred in benzene for 48 h, and the resultant yellow slurry was then centrifuged to remove the insoluble material. Toluene (4 mL) was added to the supernatant and the solution was concentrated to 4 mL before it was layered with hexane (15 mL). After 48 h at room temperature, yellow rectangular blocks of $[(Ph_2N)_2Y(\mu-NPh_2)]_2$, 2-Y, suitable for X-ray diffraction had formed.

Synthesis and Crystallization of $[(Ph_2N)_2Dy(\mu-NPh_2)]_2$, 2-Dy. In a glovebox free of coordinating solvents, $Dy[N(SiMe_3)_2]_3$ (300 mg, 0.466 mmol) was dissolved in toluene (10 mL). To the stirred solution was added HNPh₂

research communications

Table 8
Experimental details.

	1-Y	1-Er	2-Y	2-Dy	3-Er
Crystal data					
Chemical formula	$[Y(C_{12}H_{10}N)_3(C_4H_{8-}O)_2]$	$[Er(C_{12}H_{10}N)_3(C_4H_{8-}O)_2]$	$[Y_2(C_{12}H_{10}N)_6]$	$[Dy_2(C_{12}H_{10}N)_6]$	$[Er_4(C_{12}H_{10-} N)_8O_2] 2C_6H_6$
$M_{\rm r}$	737.75	816.10	1187.08	1334.26	2202.93
Crystal system, space group	Monoclinic, $P2_1/c$	Monoclinic, $P2_1/n$	Monoclinic, P2 ₁ /c	Monoclinic, $P2_1/c$	Triclinic, $P\overline{1}$
Temperature (K)	143	173	88	88	88
$a, b, c (\mathring{\mathrm{A}})$	15.3539 (9), 12.5259 (7), 20.2511 (12)	12.0946 (5), 19.1086 (8), 16.3609 (7)	9.2776 (5), 22.5591 (13), 13.4791 (8)	9.3068 (15), 22.475 (4), 13.513 (2)	12.8857 (8), 13.6846 (9), 13.7411 (9)
, β, γ (°)	90, 107.207 (1), 90	90, 91.3697 (5), 90	90, 91.4966 (9), 90	90, 91.266 (2), 90	61.3447 (8), 82.7796 (10), 83.0804 (10)
$V(\mathring{A}^3)$	3720.4 (4)	3780.1 (3)	2820.1 (3)	2825.8 (8)	2104.4 (2)
Z	4	4	2	2	1
Radiation type	Mo K	Mo K	Mo K	Mo K	Mo K
$\mu \text{ (mm}^{-1})$	1.61	2.26	2.10	2.67	4.01
Crystal size (mm)	$0.52 \times 0.38 \times 0.37$	$0.48 \times 0.39 \times 0.33$	$0.28 \times 0.24 \times 0.15$	$0.20 \times 0.12 \times 0.11$	$0.35 \times 0.28 \times 0.11$
Data collection					
Diffractometer	Bruker SMART APEXII CCD	Bruker SMART APEXII CCD	Bruker SMART APEXII CCD	Bruker SMART APEXII CCD	Bruker SMART APEXII CCD
Absorption correction	Numerical (SADABS; Krause et al, 2015)	Multi-scan (SADABS; Sheldrick, 2014b)	Multi-scan (SADABS; Krause et al, 2015)	Multi-scan (SADABS; Krause et al, 2015)	Multi-scan (TWINABS; Sheldrick, 2012)
T_{\min}, T_{\max}	0.537, 0.683	0.557, 0.695	0.622, 0.746	0.637, 0.746	0.254, 0.432
No. of measured, independent and observed $[I > 2\sigma(I)]$ reflections	42053, 8829, 7562	46529, 9687, 8834	22940, 6851, 5604	34856, 7264, 6207	51658, 10308, 9209
$R_{ m int}$	0.025	0.018	0.037	0.037	0.052
Refinement					
$R[F^2 > 2\sigma(F^2)],$ $wR(F^2), S$	0.031, 0.081, 1.04	0.019, 0.050, 1.04	0.032, 0.070, 1.03	0.026, 0.065, 1.05	0.027, 0.062, 0.96
No. of reflections	8829	9687	6851	7264	10308
No. of parameters	451	462	361	361	552
No. of restraints	0	28	0	0	0
H-atom treatment	H-atom parameters constrained	H-atom parameters constrained	H-atom parameters constrained	H-atom parameters constrained	H-atom parameters constrained
$\rho_{\rm max}$, $\rho_{\rm min}$ (e Å ⁻³)	0.81, -0.47	0.70, -0.42	0.39, -0.35	2.65, -0.81	1.62, -1.10

Computer programs: APEX2 (Bruker, 2011, 2014), SAINT (Bruker, 2009, 2013), SHELXS (Sheldrick, 2008b), SHELXT (Sheldrick, 2015a), SHELXL2014/7 (Sheldrick, 2015b) and SHELXTL (Sheldrick, 2008b).

(240 mg, 1.42 mmol) in toluene (10 mL). The resultant colorless solution was left to stir for 48 h and the color of the solution slowly turned to yellow and precipitated a yellow solid. The volatiles were removed, and the resultant yellow solids were washed with hexane. The solids were then stirred in benzene for 48 h, and the resultant yellow slurry was centrifuged to remove insoluble material. Toluene (4 mL) was added to the supernatant, and the solution was concentrated to 4 mL before it was layered with hexane (15 mL). After 48 h at room temperature, yellow rectangular blocks of $[(Ph_2N)_2Dy(\mu-NPh_2)]_2$, **2-Dy**, suitable for X-ray diffraction had formed.

Synthesis and Crystallization of {[(Ph₂N)Er(µ-NPh₂)]₄(µ-O)₂} (C₆H₆)₂, 3-Er. In a glovebox free of coordinating solvents, Er[N(SiMe₃)₂]₃ (300 mg, 0.463 mmol) was dissolved in toluene (10 mL). To the stirred solution was added HNPh₂ (240 mg, 1.41 mmol) in toluene (10 mL). The resultant colorless solution was left to stir for 48 h, and the solution slowly changed color to yellow. The volatiles were removed, and the resultant yellow solids were washed with hexane. The solids were then

stirred in benzene for 48 h, and the resultant yellow slurry was centrifuged to remove insoluble material. Toluene (4 mL) was added to the supernatant, and the solution was concentrated to 4 mL before it was layered with hexane (15 mL). After 48 h at room temperature, yellow rectangular blocks of $\{[(Ph_2N)Er(\mu-NPh_2)]_4(\mu-O)_2\}$ (C_6H_6)₂, **3-Er**, suitable for X-ray diffraction had formed. Compound **3-Er** is a minor product of a formal hydrolysis of **2-Er**, presumably from adventitious water.

6. Refinement

Refinement Details. The molecules of **2-Ln** and **3-Er** are located about an inversion center. There were two molecules of benzene solvent present per empirical formula unit in **3-Er**. Crystal data, data collection and structure refinement details are summarized in Table 8. H atoms in all five structures were placed in calculated positions and C—H bond distances were constrained to 0.95 Å for aromatic and to 0.99 Å CH₂ groups, respectively. $U_{\rm iso}({\rm H})$ values were set to $1.2U_{\rm eq}({\rm C})$.

The two tetrahydrofuran ligands in **1-Er** were modeled with disorder across two positions. For the ring of O1, two methylene groups were included in the disorder, as well as the H atoms of the remaining CH₂ groups. O-C bond distances were restrained to a target value of 1.47 (1) Å, C-C bond distances to a target value of 1.53 (1) Å. 1,3 distances between the oxygen atom and C38 and 39, and between C38B and C39B (e.g. the O-C-C angles) were restrained to be pairwise similar (with an esd of 0.02 Å). ADPs of the disordered carbon atoms (C38, C39, C38B, C39B) were constrained to be identical. U^{ij} components of ADPs of atoms C39 and C40 were restrained to be similar with an esd of 0.01 Å^2 and a distance cutoff of 4.0 Å. Subject to these conditions occupancies refined to 0.627 (12)/0.323 (12). For the ring involving O2, disorder was limited to one methylene C atom and the H atoms of the two adjacent CH₂ groups. No restraints were applied and occupancies refined to 0.633 (7)/0.367 (7).

The **3-Er** structure was found to be multi-component and was refined as a three-component twin. The orientation matrices for the three components were identified using the program $CELL_NOW$ (Sheldrick, 2008a). The second component is related to the first by no obvious twin law. The third component is related to the first by non-merohedry by a 180° rotation around $[01\overline{1}]$. The three components were integrated using SAINT (Bruker, 2013) and corrected for absorption using TWINABS (Sheldrick, 2012). The structure was solved using direct methods (Sheldrick 2008b) with only the non-overlapping reflections of main component 1. The structure was refined using all reflections of component 1 (including the overlapping reflections), resulting in minor component occupancies of 0.0615 (6) and 0.2010 (4).

Acknowledgements

We thank Jordan F. Corbey for assistance with X-ray crystallography.

Funding information

Funding for this research was provided by: National Science Foundation (grant No. CHE-1855328).

References

Addison, A. W., Rao, T. N., Reedijk, J., van Rijn, J. & Verschoor, G. C. (1984). *J. Chem. Soc. Dalton Trans.* pp. 1349–1356.

Alyea, E. C., Bradley, D. C. & Copperthwaite, R. G. (1972). J. Chem. Soc., Dalton Trans. pp. 1580–1584.

Anwander, R., Runte, O., Eppinger, J., Gerstberger, G., Herdtweck, E. & Spiegler, M. (1998). *J. Chem. Soc. Dalton Trans.* pp. 847–858.

Bienfait, A. M., Schädle, C., Maichle-Mössmer, C., Törnroos, K. W. & Anwander, R. (2014). *Dalton Trans.* 43, 17324–17332.

Bradley, D. C., Ghotra, J. S. & Hart, F. A. (1972). J. Chem. Soc. Chem. Commun. pp. 349–350.

Bradley, D. C., Ghotra, J. S. & Hart, F. A. (1973). *J. Chem. Soc. Dalton Trans.* pp. 1021–1023.

Bruker (2009, 2013). SAINT. Bruker AXS Inc., Madison, Wisconsin, USA.

Bruker (2011, 2014). APEX2. Bruker AXS Inc., Madison, Wisconsin, USA.

Coles, M. P., Hitchcock, P. B., Khvostov, A. V., Lappert, M. F., Li, Z. & Protchenko, A. V. (2010). *Dalton Trans.* **39**, 6780–6788.

Krause, L., Herbst-Irmer, R., Sheldrick, G. M. & Stalke, D. (2015). J. Appl. Cryst. 48, 3–10.

Mao, L., Shen, Q. & Jin, S. (1994). Polyhedron, 13, 1023-1025.

Meermann, C., Gerstberger, G., Spiegler, M., Törnroos, K. W. & Anwander, R. (2008). *Eur. J. Inorg. Chem.* pp. 2014–2023.

Meyer, G. & Ax, P. (1982). Mater. Res. Bull. 17, 1447-1455.

Minhas, R. K., Ma, Y., Song, J.-I. & Gambarotta, S. (1996). *Inorg. Chem.* 35, 1866–1873.

Shannon, R. D. (1976). Acta Cryst. A32, 751–767.

Sheldrick, G. M. (2008a). CELL_NOW. University of Göttingen, Germany.

Sheldrick, G. M. (2008b). Acta Cryst. A64, 112-122.

Sheldrick, G. M. (2012). TWINABS. University of Göttingen, Germany.

Sheldrick, G. M. (2015a). Acta Cryst. A71, 3-8.

Sheldrick, G. M. (2015b). Acta Cryst. C71, 3-8.

Wong, W.-K., Zhang, L., Xue, F. & Mak, T. C. W. (1997a). *Polyhedron*, **16**, 345–347.

Wong, W.-K., Zhang, L., Xue, F. & Mak, T. C. W. (1997b). *Polyhedron*, **16**, 2013–2020.

Xu, X., Yao, Y., Zhang, Y. & Shen, Q. (2007). *Inorg. Chem.* **46**, 3743–3751

Yao, Y. M., Mao, L. S., Lu, X. H., Shen, Q. & Sun, J. (2001). *J. Chin. Rare Earth Soc.* 19, 308.

Yao, Y.-Y., Lu, X., Shen, Q. & Yu, K. (2004). J. Chem. Crystallogr. 34, 275–279.

Yu, K.-X., Ding, Y.-S., Han, T., Leng, J.-D. & Zheng, Y.-Z. (2016). Inorg. Chem. Front. 3, 1028–1034.